Non-Linear Self-Interference Cancelation for Full-Duplex Transceivers Based on Hammerstein-Wiener Model

Visa Tapio, *Member, IEEE*, and Markku Juntti, *Fellow, IEEE*

***Abstract*— The main challenge in a full-duplex transceiver design is created by the self-interference caused by the coupling of the transmitted signal to the transceiver's own receiver. The effect of the non-linear operation of both the power amplifier at the transmitter and the low noise amplifier at the receiver are considered in the self-interference cancelation. The performance of three self-interference cancelers are studied: linear cancelation, auto-regressive moving-average (ARMA) based cancelation and a neural network (NN) based canceler. The NN based cancelation outperforms both the linear and ARMA based canceler but requires considerably more operations than the other two.**

***Index Terms*— Full-duplex, non-linearity, Hammerstein-Wiener model, SI-cancelation.**

I. Introduction

IN THE in-band full-duplex (FD) transmission the same carrier frequency is simultaneously used to transmit and receive data signals with the same transceiver. The main problem in a FD transceiver implementation is the self-interference (SI). The SI is caused by the coupling of the transmitted signal to the receiver input. The SI path from the transmitter to the receiver includes both the internal coupling from the transmitter output to the receiver input as well as the reflections from the environment. In order to receive the data signal from a distant signal, the SI must be attenuated to a level that is much lower than that of the desired data signal.

Since the SI signal power in the receiver input can be high, the non-linear operation of the amplifiers must be considered in the design of the SI cancelers. The SI cancelers capable to attenuate SI signals distorted by a non-linear power amplifiers (PA) have been studied, e.g., in [1]–[3]. However, since the power at the input of the low-noise amplifier (LNA) at the receiver can be high, the LNA cannot always be assumed as a linear component.

In this letter, the non-linear operation of both the PA and LNA is included in the model and three SI different techniques are used for the SI cancelation: linear cancelation, auto-regressive moving-average (ARMA) based cancelation and a neural network (NN) based canceler.

In the system model, the PA and LNA are modeled with the modified Saleh and Ghorbani models [4], [5], respectively.

Manuscript received May 23, 2021; revised July 8, 2021; accepted August 20, 2021. Date of publication September 1, 2021; date of current version November 11, 2021. This work was supported in part by the Academy of Finland 6Genesis Flagship under Grant 318927. The associate editor coordinating the review of this letter and approving it for publication was M. Oner. *(Corresponding author: Visa Tapio.)*

The authors are with the Centre for Wireless Communications (CWC), University of Oulu, 90570 Oulu, Finland (e-mail: visa.tapio@oulu.fi; markku.juntti@oulu.fi).

Digital Object Identifier 10.1109/LCOMM.2021.3109669

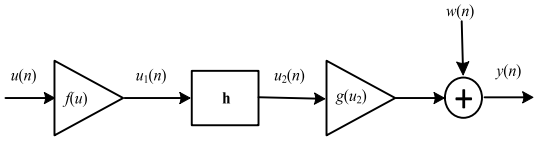

Fig. 1. Hammerstein-Wiener system.

However, it is assumed that the SI cancelers do not know the form of the non-linear function describing the non-linear operations of the amplifiers.

II. System Model

The Hammerstein-Wiener model consists of two non-linear blocks $f(u)$ and $g(u_2)$ separated by a linear block $\mathbf{h}$ as illustrated in Fig. 1. Only the input $u(n)$ and output $y(n)$ can be measured, intermediate signals $u_1(n)$ and $u_2(n)$ are not accessible for the identification.

In the full-duplex transceiver case, non-linear functions $f(u)$ and $g(u_2)$ represent the PA at the transmitter and LNA at the receiver, respectively. The linear function $h(u_1)$ describes the SI channel between the PA and LNA. It includes the direct path from PA output to the LNA input, reflections from the environment as well as the effect of the analog SI attenuation and it can be modeled as a tapped delay line. The receiver noise is added to the output signal of the non-linearity $g(u_2)$.

The baseband model for the PA can be written as

$$f(u) = G_{\text{PA}}(u)e^{j(\Phi_{\text{PA}}(u)+\phi(u))}, \tag{1}$$

where G_{PA} and $\Phi_{\text{PA}}(u)$ are the amplitude (AM-AM) and phase (AM-PM) distortions, respectively, caused by the non-linear operation of the PA and $\phi(u)$ is the phase of the input signal u. The PA can be modeled with the modified Saleh model. The amplitude and phase distortions in the modified Saleh model are given as [4]

$$G_{\text{PA}}(u) = \frac{\alpha_{\text{g}}|u|}{\sqrt{1+\beta|u|^3}} \tag{2}$$

$$\Phi_{\text{PA}}(u) = \frac{\alpha_{\Phi}}{\sqrt[3]{1+|u|^4}} - \epsilon \tag{3}$$

Similarly, the LNA can be modeled as

$$g(u_2) = G_{\text{LNA}}e^{j(\Phi(u_2)+\varphi(u_2))} \tag{4}$$

where $\varphi(u_2)$ is the phase of the signal u_2 and the AM-AM and AM-PM distortions of a LNA can be modeled with the

Ghorbani model as [5]

$$G_{\text{LNA}}(u_2) = \frac{\alpha_A |u_2^b|}{1 + b_A |u_2^c|} + d_g |u_2| \tag{5}$$

$$\Phi_{\text{LNA}}(u_2) = \frac{\alpha_{\text{LNA}} |u_2^d)|}{1 + b_\Phi |u_2^e|} + d_\Phi |u_2| \tag{6}$$

The time index n is left out from (1) – (6) to simplify the notation, i.e., $u = u(n),\ u_2 = u_2(n)$

The parameters $\alpha_{\text{g}}, \beta, \alpha_\Phi, \epsilon$ in the modified Saleh model and $\alpha_A, b, b_A, d, b_\Phi, e, c, d_\Phi$ in the Ghorbani model are used to match the models with measured amplifier characteristics. The numerical values for the parameters are given in Section IV. In the identification of the model, the non-linear functions (1) – (6) and their parameters are unknown. The length L of the linear channel $h(l)$ in (28) is assumed to be known, but the complex tap coefficients are unknown.

The noise generated in the receiver is modeled as an additive Gaussian white noise source $w(n)$ connected to the input of the LNA as shown in Fig. 1.

III. SI Cancelation

In the digital baseband SI cancelation, the SI is canceled by subtracting the replica of the SI from the input signal. The replica is formed by assuming a model for the SI channel and estimating the parameters of the model. The estimation can be done using the transmitted data signal in the half-duplex mode. After the estimation, the system can be switched to the FD mode. The SI cancelers considered in this letter are the linear, non-linear ARMA and NN based cancelers.

The functions (1) – (6) are assumed to be unknown. The commonly used baseband model for a non-linear amplifier is

$$z = \sum_{r=0}^{R-1} \alpha_t x |x|^{2t+1} \tag{7}$$

where x and z are the input and output signals of the non-linearity, R is the non-linearity order and α_t is the non-linearity coefficient.

A. Linear SI Cancelation

In the linear case, no attempt is made to estimate the non-linear functions but only the complex channel coefficients of the linear block $h(l)$ in Fig. 1 are estimated. The least squares estimate is calculated as

$$\hat{\mathbf{h}} = (\mathbf{U}^{\text{H}}\mathbf{U})\mathbf{U}^{-1}\mathbf{y} \tag{8}$$

where $\mathbf{y}$ is a vector formed from the output samples $y(n)$ and $\mathbf{U}$ is a matrix formed from input samples $u(n)$ in Fig. 1.

B. ARMA Based Cancelation

When the system in Fig. 1 is modeled with an ARMA model, the output of the system can be written as [6]

$$y(n) = -\sum_{i=1}^{P} a_i \sum_{l=1}^{q} d_l g_l^{-1}[y(n-i)] + \sum_{j=1}^{J} b_j \sum_{t=0}^{m} c_t f_t[u(n-j)] + w(n), \tag{9}$$

where a_i and b_j are the coefficients of an IIR filter used to model the linear part between the non-linear amplifiers. The first non-linearity in Fig. 1 is approximated with the model (7). Hence, functions $f_t(u)$ in (9) are

$$f_t(u) = u|u|^{2t+1} \tag{10}$$

In order to use (9), the inverse function of $g(u_2)$ is needed but it cannot be directly computed from a complex baseband non-linearity such as (7). In the ARMA model, the LNA is modeled as a third order non-linearity. In this case the inverse function can be approximated as

$$g^{-1}(y) \approx \sum_{l=0}^{1} d_l y |y|^l \tag{11}$$

i.e., functions g_l^{-1} in (9) are

$$g_l^{-1} = y|y|^l, \quad l = 0, 1. \tag{12}$$

The ARMA model can be written in matrix form as

$$\mathbf{y} = \mathbf{\Phi}_N \mathbf{x} + \mathbf{w}, \tag{13}$$

where $Y = [y(n)\ y(n+1) \cdots y(n+N-1)]^{\text{T}}$ is the output vector and $\mathbf{w}$ is the noise vector. The known matrix $\Phi_N = [\Phi(1) \cdots \Phi(N)]^{\text{T}}$ consists of vectors

$$\begin{aligned}\Phi(n) = [&f_1[u(n)] \cdots f_m[u(n)] \cdots f_1[u(n-J)] \\ &\cdots f_m[u(n-J)]\ g_1^{-1}[y(n-1)] \cdots g_q^{-1}[y(n-1)] \\ &\cdots g_1^{-1}[y(n-P)] \cdots g_q^{-1}[y(n-P)]\end{aligned} \tag{14}$$

The unknown vector is

$$\begin{aligned}\mathbf{x} = [&b_1 c_1 \cdots b_1 c_m\ b_2 c_1 \cdots b_2 c_m\ b_n c_1 \cdots b_n c_m \\ &a_1 d_1 \cdots a_1 d_q\ a_2 d_1 \cdots a_2 d_q\ a_p d_1 \cdots a_p d_q]\end{aligned} \tag{15}$$

The output of the ARMA model in (13) is a linear function of the elements in (15). In system identification problems, e.g. in [6], the goal is to find an estimate for all the unknown parameters $a_i,\ b_j,\ c_t$ and d_l. However, in the SI cancelation, the goal is to generate a replica of the SI signal. Hence, the parameter separation needed in the system identification is not necessary in this case. This simplifies the estimation task. The vector $\mathbf{x}$ can be solved with linear estimation methods. The least mean square (LMS) iteration for the vector $\mathbf{x}$ is

$$\mathbf{w}(k+1) = \mathbf{w}(k) - \mu \mathbf{\Delta} e(k), \tag{16}$$

where $\Delta = \Phi(k)^*$, μ is the iteration step size and $e(k) = y(k) - \hat{y}(k)$ is the estimation error at iteration k.

C. Neural Network Based Cancelation

Neural networks have been proposed for SI cancelation in [7] and [8] wherein the PA non-linearity and transmitter IQ imbalance is considered but the LNA is assumed to be linear. In [7], the SI canceler uses time-delay NN, while in [8], the NN based SI cancellers are constructed as a ladder-wise grid and moving-widow grid structures. Both [7] and [8] employ rectified linear activation units as activation functions.

Here, the NN based cancelation is applied in the case where both the PA and LNA are operating at their non-linear regime

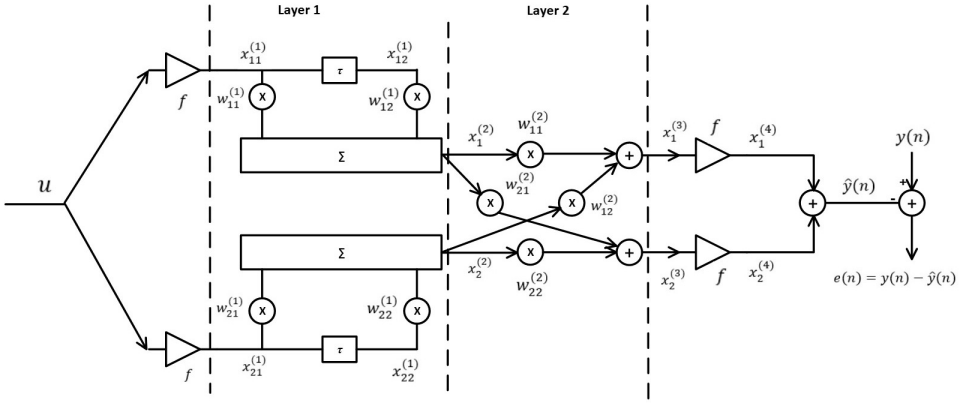

Fig. 2. Neural network model.

due to the strong SI. The NN structure is presented in Fig. 2. The motivation for the structure is the Hammerstein-Wiener model in Fig. 1, where a linear filter is between two non-linear functions. Hence, an intuitive solution is to construct the NN with non-linear input nodes, followed by linear tapped delay lines and non-linear functions at the output. Only two parallel branches are shown in the figure. Using the notation in Fig. 2, the output of the network can be written as

$$y(n) = \sum_{n=1}^{N} x_n^{(4)} = \sum_{n=1}^{N} f(x_n^{(3)}), \tag{17}$$

where N is the number of the parallel branches of the network and the activation function f is defined as

$$f(k) = f_{\text{Re}}(\text{Re}\{x_n^{(3)}\}) + j f_{\text{Im}}(\text{Im}\{x_n^{(3)}\}). \tag{18}$$

Functions $f_{\text{Re}}(s)$ and $f_{\text{Im}}(s)$ are identical for all $s \in \mathbb{R}$.

$$f_{\text{Re}}(s) = f_{\text{Im}}(s) = \frac{b}{1+e^{-as}} - \frac{1}{2} \tag{19}$$

By collecting the internal signals $x_n^{(3)}$ to a vector, they can be given in a matrix form as

$$\mathbf{x}^{(3)} = \mathbf{W}^{(2)}\mathbf{W}^{(1)}\mathbf{x}^{(1)}, \tag{20}$$

where the coefficients of Layer 2 are collected to matrix

$$\mathbf{W}^{(2)} = \begin{pmatrix} w_{11}^{(2)} & \cdots & w_{1N}^{(2)} \\ \vdots & \cdots & \vdots \\ w_{N1}^{(2)} & \cdots & w_{NN}^{(2)} \end{pmatrix} \tag{21}$$

and the coefficient matrix for Layer 1 is

$$\mathbf{W}^{(1)} = \begin{pmatrix} \mathbf{w}_1^{(1)} & \mathbf{0} & \mathbf{0} & \cdots & \mathbf{0} \\ \mathbf{0} & \mathbf{w}_2^{(1)} & \mathbf{0} & \cdots & \mathbf{0} \\ \vdots & \vdots & \vdots & \vdots & \vdots \\ \mathbf{0} & \cdots & \mathbf{0} & \mathbf{w}_{N-1}^{(1)} & \mathbf{0} \\ \mathbf{0} & \mathbf{0} & \cdots & 0 & \mathbf{w}_N^{(1)} \end{pmatrix} \tag{22}$$

where $\mathbf{w}_n^{(1)} = [w_{n1}^{(1)}\ w_{n1}^{(1)}\ \cdots\ w_{nT}^{(1)}]$ and $\mathbf{0}$ is a row vector of length T whose elements are zeros. Vector $\mathbf{x}^{(1)}$ is given as $\mathbf{x}^{(1)} = [x_{11}^{(1)}\ \cdots\ x_{1T}^{(1)}\ x_{21}^{(1)}\ \cdots\ x_{21}^{(1)}\ x_{2T}^{(1)}\ \cdots\ x_{N1}^{(1)}\ \cdots\ x_{NT}^{(1)}]^{\text{T}}$ and $x_{ij}^{(1)} = f(u(n-j),\ j = 0 \cdots T-1$, where T is the length of the tapped delay lines in Fig. 2.

Coefficients $w_{ij}^{(n)}$ can be solved iteratively over the layers by the back-propagation algorithm as

$$w_{ij}^{(n)} = w_{ij}^{(n-1)} - \mu\left(\frac{\partial E}{\partial \text{Re}\{w_{ij}^{(n-1)}\}} + j\frac{\partial E}{\partial \text{Im}\{w_{ij}^{(n-1)}\}}\right) \tag{23}$$

The partial derivatives for the layer 2 are

$$\begin{aligned} &\frac{\partial E}{\partial \text{Re}(w_{ij}^{(2)})} \\ &\quad = -2(\text{Re}(y)) - \text{Re}(\hat{y}))f'[\text{Re}(x_i^{(4)})]\text{Re}(x_j^{(2)}) \\ &\qquad - 2(\text{Im}(y)) - \text{Im}(\hat{y}))f'[\text{Im}(x_i^{(4)})]\text{Im}(x_j)^{(2)} \end{aligned} \tag{24}$$

$$\begin{aligned} &\frac{\partial E}{\partial \text{Im}(w_{ij}^{(2)})} \\ &\quad = -2(\text{Re}(y)) - \text{Re}(\hat{y}))f'[\text{Re}(x_i^{(4)})]\text{Im}(x_j^{(2)}) \\ &\qquad + 2(\text{Im}(y)) - \text{Im}(\hat{y}))f'[\text{Im}(x_i^{(4)})]\text{Re}(x_j^{(2)}) \end{aligned} \tag{25}$$

The partial derivatives for the layer 1 coefficients are

$$\begin{aligned} &\frac{\partial E}{\partial \text{Re}(w_{ij}^{(1)})} \\ &\quad = -2(\text{Re}(y)) - \text{Re}(\hat{y}))\sum_{k=1}^{N}\text{Re}\{w_{kj}^{(2)}x_{ij}^{(1)}\}f'[\text{Re}(x_k^{(4)})] \\ &\qquad - 2(\text{Im}(y)) - \text{Im}(\hat{y}))\sum_{k=1}^{N}\text{Im}\{w_{kj}^{(2)}x_{ij}^{(1)}\}f'[\text{Im}(x_k^{(4)})] \end{aligned} \tag{26}$$

$$\begin{aligned} &\frac{\partial E}{\partial \text{Im}(w_{ij}^{(1)})} \\ &\quad = -2(\text{Re}(y)) - \text{Re}(\hat{y}))\sum_{k=1}^{N}\text{Im}\{w_{kj}^{(2)}x_{ij}^{(1)}\}f'[\text{Re}(x_k^{(4)})] \\ &\qquad + 2(\text{Re}(y)) - \text{Im}(\hat{y}))\sum_{k=1}^{N}\text{Im}\{w_{kj}^{(2)}x_{ij}^{(1)}\}f'[\text{Im}(x_k^{(4)})] \end{aligned} \tag{27}$$

IV. Numerical Results

The signal used in the numerical examples is a LTE downlink signal with 20 MHz bandwidth generated with a transmitter model available in MathWorks Matlab LTE

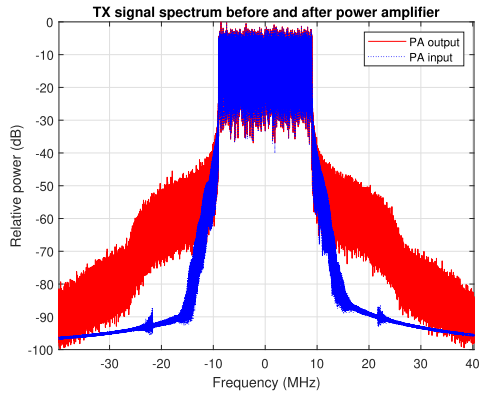

Fig. 3. The spectrum of the transmitted signal.

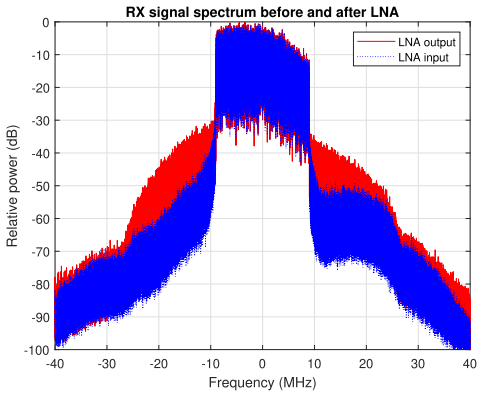

Fig. 4. The spectrum of the received signal.

TABLE I
PA AND LNA MODEL PARAMETERS

PA		LNA			
α_g	1.0536	α_a	1.92	d_g	0
β	0.08594	b	1.0	α_{LNA}	0.023
α_Φ	0.161	b_A	0.46	d	6
ϵ	7.1	c	3.0	b_Φ	0.1
				e	2
				d_Φ	0

Toolbox. The signal is first generated with a sample rate of 30.72 Msamples/s. The signal is then up-sampled by a factor 4. The up-sampled signal is filtered to reduce the power at adjacent channels. After the filtering, the signal is amplified with a non-linear PA modeled with the modified Saleh model as described in Section II. The PA parameters are given in Table I and they are used to model a solid-state power amplifier [9]. The spectrum of the transmitted signal before and after the PA is shown in Fig. 3. The adjacent channel power ratio (ACPR) of the transmitted signal after the PA is -44 dB which is close to the requirement of -45 dB for a LTE base station [10].

After the PA, the signal is transmitted through the linear SI channel. The SI channel is modeled with a tapped delay line as

$$u_2(n) = \sum_{l=0}^{L-1} h(l) u_1(n-l) \tag{28}$$

where $h(l)$ is the l^{th} complex tap coefficient of the SI channel (l^{th} element of the channel vector $\mathbf{h}$ in Fig. 1) and L is the length of the channel. The length of the channel in simulations is $L = 3$ and time delays are 0, 32.55 and 65.1 ns. These correspond to reflections from 0, 4.875 and 9.765 meters distance, assuming the signal is reflected only once. The output signal of the linear channel is amplified with the LNA. The LNA is modeled with the Ghorbani model discussed in Section II. The parameters for the LNA model given in Table I represent a class-A amplifier [5]. An example spectrum before (blue) and after (red) LNA is shown in Fig. 4. The spectra in Fig. 4 are calculated without noise. The output of the LNA is down-sampled by a factor 4. The SI cancelation is done for the down-sampled signal using techniques described in Section III.

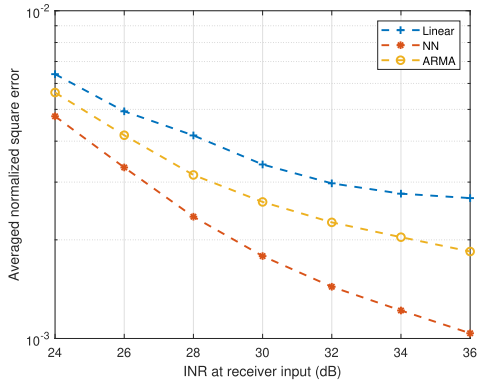

Fig. 5. Averaged normalized squared error when noise added after the LNA.

The same numbers of samples (3000) are used for all three SI cancelation techniques in the training phase to allow a fair comparison of their performance. The total number of samples transmitted during one channel realization is 307200 resulting in the training–validation ratio of 0.01. The number of parallel branches in the NN based SI cancelation was selected by experiments to be 11. The performances of the SI cancelers are averaged over 300 SI channel realizations. The normalised averaged squared errors of the SI estimates are shown in Fig. 5. The interference-to-noise ratio (INR) after the cancelation is shown in Fig. 6. At low INR values, the non-linear distortion is below the noise level and all considered cancelers are able to cancel the SI signal. When the INR increases the distortion starts to affect the performance and the NN starts to outperform both the LS and the ARMA based cancelers. E.g., the output INR after the cancelation reaches 2 dB when the INR at the input before cancelation is 24 dB, 26 dB and 29 dB with LS, ARMA and NN cancelers, respectively.

In Figs. 5 and 6 the noise is added to the signal after the LNA. Since a small part of noise is generated also before the LNA and inside of it, a case where the noise is added before the LNA and is hence amplified by the LNA is also considered. When the INR is above 30 dB, the performance in this case is the same as in the case where noise is added after the LNA.

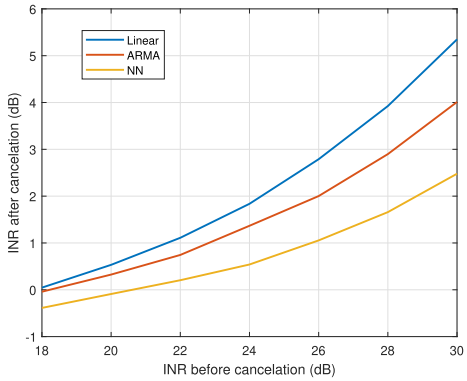

Fig. 6. Interference-to-noise ratio when noise added after LNA.

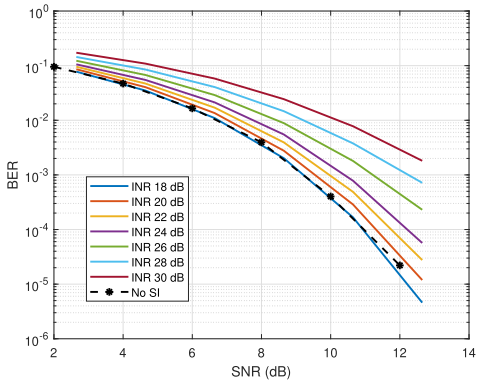

Fig. 7. Bit-error-rate when SI is canceled with the neural network.

When INR is below 30 dB, the SI cancelation performance in the case where the noise is added after the noise is 0.5 dB better than in the case where the noise is amplified by the non-linear LNA.

The bit-error-rate (BER) performance with a QPSK modulated LTE signal is simulated in a case where the relative delays and powers of the channel taps between the distant transmitter and receiver are 0, 8.14 and 73.24 ns and 0, −10 and −21 dB, respectively. The BER with the NN based SI canceler is shown in Fig. 7. The values at the horizontal axis give the signal-to-noise (SNR) ratio of the desired data signal transmitted by a distant transmitter. Cases where the INR before the SI canceler is 18 – 30 dB are shown with curves labeled as 'INR 18 dB' – 'INR 30 dB'. The curve labeled as 'No SI' shows the reference BER performance when no SI is present in the system. The computational complexities of the SI cancelers shown in Table II are assessed by calculating the number of real-valued operations required at each iteration during the training phase. The number of operations for the LS based canceler is calculated assuming that the LS problem is solved with the singular value decomposition. The number of operations for the ARMA based canceler is calculated from (10) – (16) and for the NN based canceler from (23) – (27).

TABLE II
COMPUTATIONAL COMPLEXITY AT EACH ITERATION DURING THE TRAINING

LS	$64L^3 + 80L^2$
ARMA	$27L + 3$
NN	$52LN^2 + 40N^2 + 12LN + 3$

V. CONCLUSION

The PA and LNA of a FD transceiver were modeled with the modified Saleh and Ghorbani models, respectively. However, the form of non-linearity cannot be fully known in a FD transceiver. Hence, in the considered SI cancelation techniques the non-linearities were assumed to be unknown. Three different approaches for the SI cancelation were compared: linear cancelation, ARMA based cancelation and NN based cancelation. The NN based cancelation gives the best performance. It has considerably higher computational complexity than the two other SI cancelers considered in this letter. The acceptable balance between the performance and the computational complexity varies from one application to another, but the complexity – performance trade-off is not analyzed here. The ARMA based canceler would work well if the non-linear functions were known, i.e., the PA and LNA would follow the simplified memory-less non-linear model in (7). The PA and LNA models in (2) – (6) are based on the measurements and the memory effects of the amplifiers contribute to the models. Since these can vary in time and temperature, they cannot be fully known and the NN approach is needed to attain adequate performance.

REFERENCES

[1] D. Korpi, Y.-S. Choi, T. Huusari, L. Anttila, S. Talwar, and M. Valkama, "Adaptive nonlinear digital self-interference cancellation for mobile inband full-duplex radio: Algorithms and RF measurements," in *Proc. IEEE GLOBECOM*, Dec. 2015, pp. 1–7.

[2] D. Korpi, T. Huusari, Y.-S. Choi, L. Anttila, S. Talwar, and M. Valkama, "Digital self-interference cancellation under nonideal RF components: Advanced algorithms and measured performance," in *Proc. IEEE 16th Int. Workshop Signal Process. Adv. Wireless Commun. (SPAWC)*, Jun. 2015, pp. 286–290.

[3] V. Tapio, M. Sonkki, and M. Juntti, "Self-interference cancelation in the presence of non-linear power amplifier and receiver IQ imbalance," *EURASIP J. Wireless Commun. Netw.*, vol. 2020, no. 1, pp. 1–21, Dec. 2020, doi: 10.1186/s13638-020-01743-z.

[4] M. O'Droma, S. Meza, and Y. Lei, "New modified Saleh models for memoryless nonlinear power amplifier behavioural modelling," *IEEE Commun. Lett.*, vol. 13, no. 6, pp. 399–401, Jun. 2009.

[5] I. Teikari, "Digital predistortion linearization methods for RF power amplifiers," Ph.D. dissertation, Helsinki Univ. Technol., Espoo, Finland, 2008. [Online]. Available: http://lib.tkk.fi/Diss/2008/isbn9789512295463.pdf

[6] E.-W. Bai, "An optimal two-stage identification algorithm for Hammerstein–Wiener nonlinear systems," *Automatica*, vol. 34, no. 3, pp. 333–338, Mar. 1998.

[7] Y. Kurzo, A. Burg, and A. Balatsoukas-Stimming, "Design and implementation of a neural network aided self-interference cancellation scheme for full-duplex radios," in *Proc. 52nd Asilomar Conf. Signals, Syst., Comput.*, Oct. 2018, pp. 589–593.

[8] M. Elsayed, A. A. A. El-Banna, O. A. Dobre, W. Shiu, and P. Wang, "Low complexity neural network structures for self-interference cancellation in full-duplex radio," *IEEE Commun. Lett.*, vol. 25, no. 1, pp. 181–185, Jan. 2021.

[9] D. Schreurs, M. O'Droma, A. A. Goacher, and M. Gadringer, Eds., *RF Power Amplifier Behavioral Modeling*. Cambridge, U.K.: Cambridge Univ. Press, 2008.

[10] *LTE; Evolved Universal Terrestrial Radio Access (E-UTRA); Base Station (BS) Radio Transmission and Reception (Version 16.7.0 Release 16)*, document TS 36.104, ETSI, Tech. Rep., Nov. 2020.